JOURNAL OF CATALYSIS **178,** 640–648 (1998)
ARTICLE NO. CA982193

Characterization of Vanadia Sites in V-Silicalite, Vanadia-Silica Cogel, and Silica-Supported Vanadia Catalysts: X-Ray Powder Diffraction, Raman Spectroscopy, Solid-State ^{51}V NMR, Temperature-Programmed Reduction, and Methanol Oxidation Studies

Chuan-Bao Wang, Goutam Deo,[1] and Israel E. Wachs[2]

Zettlemoyer Center for Surface Studies and Department of Chemical Engineering, Lehigh University, Bethlehem, Pennsylvania 18015

Received February 16, 1998; revised June 11, 1998; accepted June 22, 1998

The vanadia species in different silica environments (silicalite, cogel, and silica-supported) were characterized by XRD, Raman, solid state ^{51}V NMR, TPR, and methanol oxidation. Under dehydrated conditions, the dispersed vanadia species in all of the vanadia-silica systems possess an isolated and distorted VO_4 coordination with minor differences. The VO_4 species in the dehydrated 1% silica-supported vanadia catalyst contains a single terminal V=O bond and changes coordination from VO_4 to VO_5 or VO_6 upon hydration. The VO_4 species in the V-silicalite maintains its coordination upon hydration and essentially does not appear to possess a terminal V=O bond. A trace amount of crystalline V_2O_5 and two types of dispersed VO_4 species are present in the 1% vanadia-silica cogel. One of the dispersed VO_4 species is a surface vanadia species on silica and changes coordination upon hydration. All of the dispersed vanadia species exhibit similar reducibility and catalytic properties for methanol oxidation because they possess very similar V-O-Si bridging bonds that are the critical functionalities for methanol oxidation.

INTRODUCTION

Vanadium oxide in different silica environments has a variety of potential applications in both chemical and environmental industries. Vanadia supported on silica exhibits unique catalytic properties for selective oxidation of hydrocarbons to oxygenates and olefins (1–5). V-silicalites with the MFI structure have been intensively investigated for selective oxidation of hydrocarbons and primary amines (6–9), ammoxidation (10,11), selective catalytic reduction (SCR) of NO_x (12), and liquid-phase oxidation with H_2O_2 (13,14). Vanadia-silica cogels exhibit high activity and stability for SCR of NO_x (15) and high activity for selective oxidation of methane to formaldehyde and methanol (16).

The vanadia species in the above three different types of silica environments have been characterized by various techniques: Raman, EXAFS/XANES, ^{51}V NMR, and photoluminescence. The vanadia species supported on silica has been proposed to exist as an isolated and distorted VO_4 species with a single V=O terminal bond and three bridging bonds connected to the silica support (17–20). Upon hydration, the surface vanadia species on SiO_2 changes coordination from VO_4 to VO_5 or VO_6. The vanadia species in V-silicalites with the MFI structure has been reported to contain V^{5+} in VO_4 coordination (21,22). The vanadia species in vanadia-silica cogels was identified to contain two types of VO_4 species (16,23): one changes coordination upon hydration, suggesting that it is an accessible vanadia site; and the other does not change coordination upon hydration, suggesting that it is an inaccessible vanadia site.

The purpose of the present work is to further investigate the differences and similarities of the vanadia species in the different silica environments and to investigate the impact, if any, of the different vanadia species on the structure-reactivity relationships of these catalysts. The structure of the different vanadia sites was determined from solid state ^{51}V NMR and Raman spectroscopy, and the reducibility and reactivity were probed with temperature-programmed reduction and methanol oxidation. The structure–reactivity relationships should provide fundamental information on the effect of the different silica environments on the properties of the vanadia sites.

EXPERIMENTAL

Catalyst Preparation

The V-silicalite was synthesized using tetraethoxysilane (TEOS, Janssen Chimica) as the silicon source and $VOSO_4 \cdot 5H_2O$ (Janssen Chimica) as the vanadium source with a V/Si molar ratio = 0.0200 in the synthesis gel. Hydrothermal crystallization was carried out in a Teflon-lined

[1] On leave from Department of Chemical Engineering, Indian Institute of Technology, Kanpur, India.

[2] Corresponding author. E-mail: IEW0@LEHIGH.EDU.

0021-9517/98 $25.00

autoclave under a nitrogen atmosphere at 180°C for three days. The V/Si molar ratio in the as-synthesized zeolite was determined by ICP analysis to be 0.0101 (equivalent to 1.5 wt% V_2O_5).

A 1 wt% silica-supported vanadia catalyst, designated as 1% silica-supported, was prepared by impregnating a fused Cab-O-Sil silica support (Cabot EH-5, 380 m^2/g) with a methanol solution of vanadium triisopropoxide oxide (Alfa, 95–98%) in a nitrogen atmosphere. The sample was initially dried at room temperature for 2 h and further dried at 120°C overnight in N_2 flow and subsequently calcined at 500°C for 6 h in O_2 flow.

A 1 wt% vanadia-silica cogel catalyst, designated as 1% cogel, was synthesized using a two-step sol–gel process with tetraethoxysilane (TEOS, Fisher) and vanadium triisopropoxide oxide (VTPO, Fisher) as the precursors (16). The SiO_2 sol was first prepared by combining TEOS in methanol with diluted nitric acid. Then the mixed V_2O_5-SiO_2 sol was obtained by adding VTPO (diluted in methanol) into the SiO_2 sol. The molar ratio of TEOS/methanol/nitric acid/H_2O is 1.0/2.8/0.7/7.8, while an appropriate amount of VTPO was utilized to give vanadium content corresponding to 1 wt% V_2O_5 in the final cogel product. The gel formed with 12 h and then allowed to age for another 10 h. All the above operations were carried out at ambient temperature. The obtained gel was dried at 50°C for 15 h, 120°C for 5 h, and calcined at 550°C for 4 h in air. The final 1 wt% vanadia-silica cogel possesses a BET surface area of 509 m^2/g.

X-Ray Powder Diffraction

XRD patterns were obtained with a Philips APD 1700 automated powder diffractometer with nickel-filtered CuKα radiation ($\lambda = 0.1542$ nm) and X-ray generator setting at 45 kV and 30 mA. The scan rate and angle increment were 2.0 degree/min and 0.03 degree, respectively.

Raman Spectroscopy

Two Raman spectrometers were used in this work. Both of them consisted of a Spex triplemate spectrometer (Model 1877). Prior to Raman analysis, all of the samples were heated at 600°C for 1 h in air to diminish fluorescence.

One of the spectrometers, equipped with an Ar^+ laser (Spectra Physics, Model 165), a Princeton Applied Research OMA III optical multichannel photodiode array detector (Model 1420), and a rotating *in situ* cell as described in Ref. (24), was used for obtaining the Raman spectra of the V-silicalite catalyst under dehydrated conditions. A thin wafer of about 200–300 mg of the sample was placed into the *in-situ* cell, heated to 600°C for 1 h and cooled to 50°C in O_2 flow (Ultra High Purity, Linde, 100-200 ml/min) to obtain the Raman spectra under dehydrated conditions.

The other spectrometer, equipped with an Ar^+ laser (Spectra Physics, Model 164) and a Princeton Applied Research OMA III optical multichannel photodiode array detector (Model 1421), was used for obtaining the Raman spectra of vanadia-silica cogel and silica-supported vanadia catalysts under dehydrated conditions by heating each sample at 450°C for 0.5 h with flowing O_2 and then cooled down to ~50°C in a stationary *in situ* cell as described in Ref. (25).

The latter spectrometer was also used for obtaining all the Raman spectra under hydrated conditions. Hydration of vanadia-silica cogel and silica-supported vanadia catalysts was achieved by exposing the dehydrated samples to ambient air for 2 days. The V-silicalite was hydrated by depositing water drops onto the thin wafer since the V-silicalite sample in air or in a desiccator containing moisture for a short time would exhibit strong fluorescence.

Solid State ^{51}V NMR Spectroscopy

Two General Electric GN-300 spectrometers, equipped with a Nicolet fast digitizer and a MAS Doty probe, were used for this study. One of the spectrometers was utilized to obtain the NMR spectra of the V-silicalite and silica-supported vanadia catalysts. Wide-line ^{51}V NMR studies were carried out at 79.0 MHz using a θ-τ-θ spin echo sequence with a delay time $\tau = 50$ μs, a solid flip angle close to 45°, and a relaxation delay of 0.2–1 s. Magic-angle spinning (MAS) spectra were obtained at spinning speeds of 8–9 kHz. The spectra under dehydrated conditions were measured by sealing the samples within ampoules after dehydration at 400°C in a vacuum of 10^{-3} Torr, followed by O_2 reoxidation at 400°C for 1 h.

The other spectrometer was used for obtaining the wide-line ^{51}V NMR spectra of the vanadia-silica cogel catalyst (16). The measurement was carried out on a static sample with a simple one-pulse excitation of 1 μs width, a preaquisition delay of 10 μs, a dwell time of 0.5 μs, and a relaxation of 5–10 s. Dehydrated xerogel samples were achieved by calcination at 550°C for 4 h, cooling in a desiccator over dehydrated 4 A zeolite, followed by transferring and sealing to an NMR sample tube in a glove box under dry N_2 flow.

Hydration of all the samples was achieved by exposing them to ambient air for 2 days.

Temperature-Programmed Reduction (TPR)

Temperature-programmed reduction was carried out in an Altamira AMI-100 system. The catalyst samples (60–120 mg) were loaded in a quartz U-tube reactor and pretreated at 500°C for 1 h in flowing dry air. TPR profiles were obtained under the following conditions: flow rate, 30 ml/min; reducing gas, 10% hydrogen in argon; heating rate, 10°C/min. The H_2 consumption was monitored using a TCD.

Methanol Oxidation Studies

Methanol oxidation was carried out in a fixed-bed reactor at atmospheric pressure and 380°C. The details about the reactor system have been previously described (26). The amount of the catalysts was varied in the range of 15–45 mg in order to achieve a methanol conversion of ~10 mol%. A gas mixture of methanol/O_2/He = 6/11/83 was used as the feed with a total flow rate of 50 ml/min. An HP GC (Model 5890 II) equipped with TCD and FID detectors was used to analyze the reactants and products.

RESULTS

XRD Patterns

The XRD patterns of the 1% silica-supported and 1% cogel catalysts showed only a broad peak characteristic of amorphous silica (shown in Fig. 1), indicating that the vanadium is a highly dispersed state or the vanadia crystals are too small (<4 nm) to be detected by XRD.

The XRD pattern of the V-silicalite sample reveals that all the diffraction peaks correspond to those of pure silicalite with the MFI structure (27), and V_2O_5 crystallites, as well as other crystalline phases, are absent. The most intense reflections in the V-silicalite are in the $23^\circ < 2\theta < 25^\circ$ region, whereas in pure silicalite the most intense reflections are in the $5^\circ < 2\theta < 10^\circ$ region (27). The cell parameters of the V-silicalite were found to be a = 20.10, b = 19.85, and c = 13.38 Å, which are slightly higher than those for pure silicalite (27b). This observation is in good agreement with the results of V-silicalites reported in Ref. (22). The relatively poorer XRD pattern of the V-silicalite is related to its small crystal size (0.2–0.5 μm).

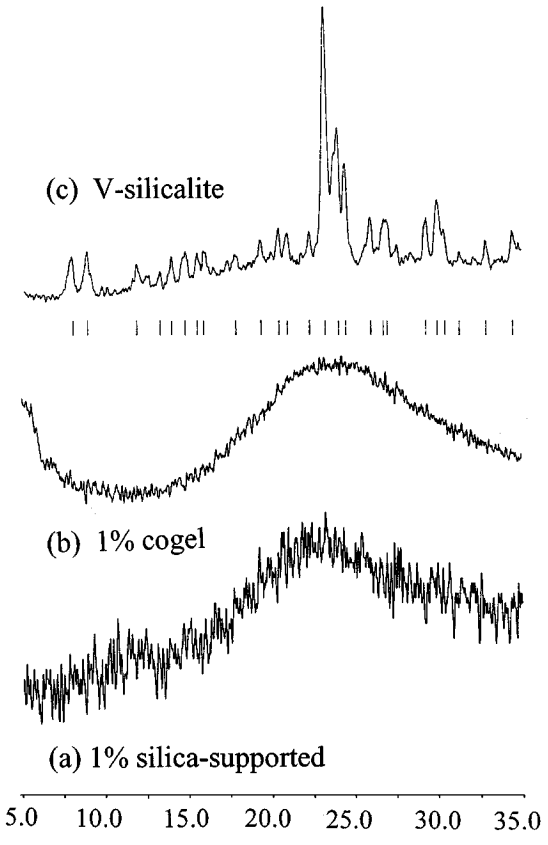

FIG. 1. X-ray diffraction patterns of (a) 1%-supported V_2O_5/SiO_2, (b) 1% V_2O_5-SiO_2 cogel, and (c) V-silicalite.

Raman Spectra

The Raman spectra of the 1% silica-supported vanadia catalyst were reported elsewhere along with extensive discussion (18). The silica support gives vibrations at 485, 600, 800, and 975 cm^{-1}. Under dehydrated conditions, a sharp Raman band at 1037 cm^{-1} was present, which is characteristic of the terminal V=O bond of a surface VO_4 species. In addition, two weak Raman bands at 1080 and 910 cm^{-1} are characteristic of Si-O^- and Si(-O^-)$_2$ functionalities (18). Under hydrated conditions, the vanadium oxide on silica surface gives rise to Raman bands at 150, 263, 323, 418, 512, 670–700, and 990–1016 cm^{-1}, characteristic of a hydrated surface vanadia species on silica. The 1016 band is characteristic of a terminal V=O bond in the surface vanadia species that is partially dehydrated by the laser beam. The Raman bands at 200–300 and 500–800 cm^{-1} are assigned to V-O-V vibrations, and the Raman band at 150 cm^{-1} is due to a lattice vibration.

The Raman spectrum of the V-silicalite under dehydrated conditions in the 700–1100 cm^{-1} region is shown in Fig. 2A. The Raman spectra of dehydrated Ti-silicalite and pure silicalite are also shown in Fig. 2A for comparison. The Raman spectra in the 200–700 region are not shown because there is little difference for the silicalite, V-silicalite, and Ti-silicalite samples. The V-silicalite sample possesses an intense Raman band at 956 cm^{-1}, which is downshifted with respect to the 972 cm^{-1} band of the pure silicalite. The Ti-silicalite sample possesses a Raman band at 955 cm^{-1}, which is similar to the V-silicalite sample. The 955/956 cm^{-1} Raman band of the V-silicalite and Ti-silicalite samples are much more intense than the 972 cm^{-1} band of the pure silicalite. The Raman spectrum of the V-silicalite shows an additional very weak feature at 1034 cm^{-1}. In contrast to the silica-supported catalyst, the Raman spectrum of the V-silicalite exhibits little change upon hydration, shown in Fig. 2B.

The Raman spectra of the dehydrated and hydrated 1% vanadia-silica cogel catalyst are presented in Fig. 3. The cogel sample possesses a trace amount of crystalline V_2O_5, evidenced by the presence of Raman bands at 141, 280, ~402, ~485, ~525, ~700, and 992 cm^{-1} in Fig. 3a. Similar to the Raman spectrum of the 1% silica-supported vanadia catalyst, the Raman band at 1033 cm^{-1} due to the terminal V=O bond and the Raman bands at 485, 600, 800, and

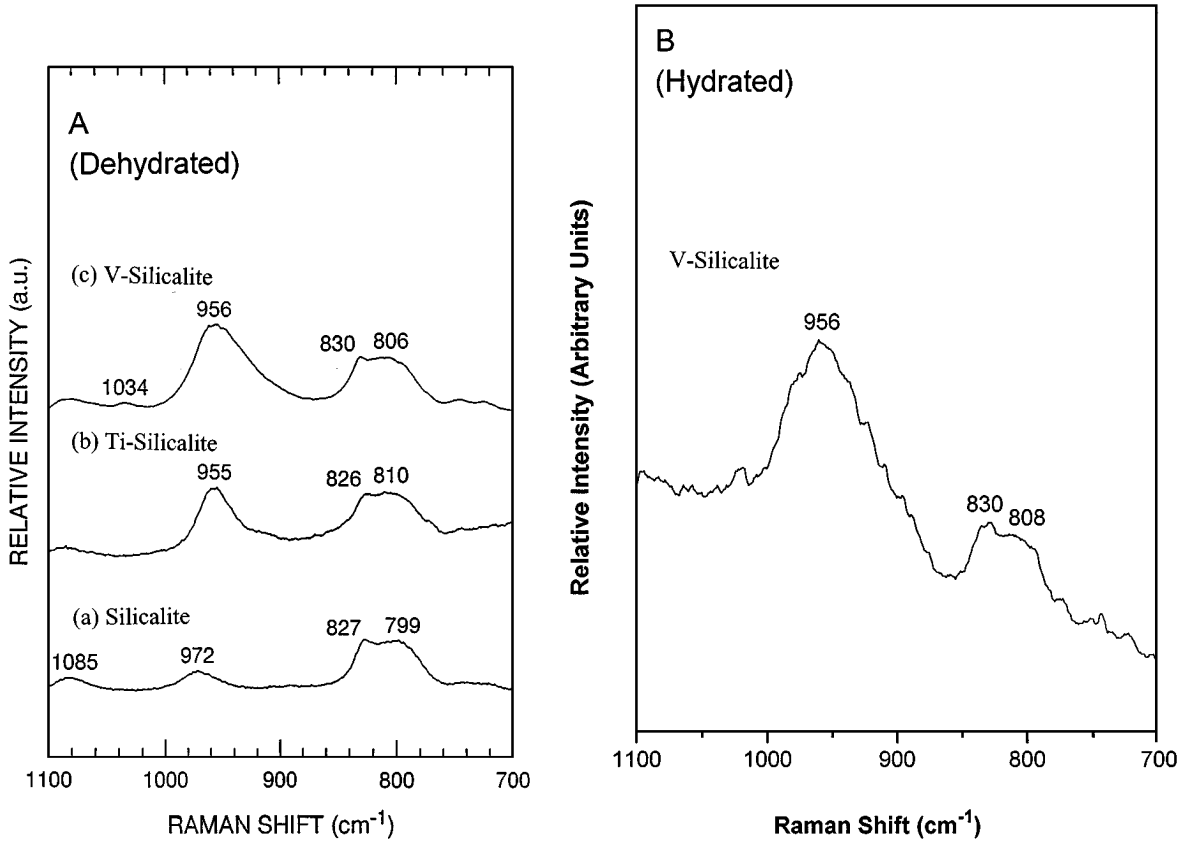

FIG. 2. Raman spectra of (a) silicalite, (b) Ti-silicalite, and (a) V-silicalite catalysts under dehydrated (A) and hydrated (B) conditions.

975 cm^{-1} due to the silica support were also observed under dehydrated conditions. In addition, the weak Raman bands at 1080 and 910 cm^{-1} due to the Si-O^- and Si(-O^-)$_2$ functionalities were also present (18). Under hydrated conditions, Raman bands of the cogel sample were observed at 150, ~260, 310, 410, 520, 648–761, and 990–1016 cm^{-1}, which are characteristic of the hydrated surface vanadia species on silica similar to that in the silica-supported vanadia catalyst (18, 28). This implies that the vanadia species in the cogel sample also interacts with moisture to form the hydrated surface vanadia species.

Solid State ^{51}V NMR Spectra

The ^{51}V NMR wide-line and MAS spectra of the V-silicalite sample under dehydrated and hydrated conditions are presented in Fig. 4. Only a broad line centered at −586 ppm, characteristic of an asymmetric chemical shift tensor with components of −370, −580, and −950 ppm, is present under dehydrated conditions (Fig. 4a). Compared to the reference spectra of model compounds with well-defined coordination (29,30), the line of the V-silicalite can be assigned to the presence of V^{+5} in a highly distorted VO_4 coordination. No features at ~−280 and ~−1300 ppm are present, indicating the absence of crystalline V_2O_5. The ^{51}V MAS NMR spectrum of the V-silicalite possesses only a single set of side bands with an isotropic chemical shift of −610 ppm, indicative of only one type of V site. Subsequent exposure to ambient conditions results in little change in the line shape and position (Fig. 4b), strongly suggesting that there is no coordination change upon hydration.

The chemical shift parameters of the V-silicalite, vanadia-silica cogel, and silica-supported vanadia catalysts under dehydrated conditions are summarized in Table 1.

TABLE 1

^{51}V Chemical Shift Parameters Observed for the V-Silicalite, Vanadia-Silica Cogel, and Silica-Supported Vanadia Catalysts under Dehydrated Conditions

Sample	Line position (ppm)	δ_1 (ppm)	δ_2 (ppm)	δ_3 (ppm)	δ_{iso} (ppm)
10% supported	−510	−450[a]	−470[a]	−1190[a]	−710[c]
1% cogel	−510	−460[b]	−500[b]	−850[b]	−603[d]
V-silicalite	−586	−370[a]	−580[a]	−950[a]	−610[c]

[a] The values obtained from simulated wide-line spectra.
[b] The values estimated from wide-line spectra.
[c] The values measured from MAS spectra.
[d] The value calculated as $\delta_{iso} = 1/3(\delta_1 + \delta_2 + \delta_3)$.

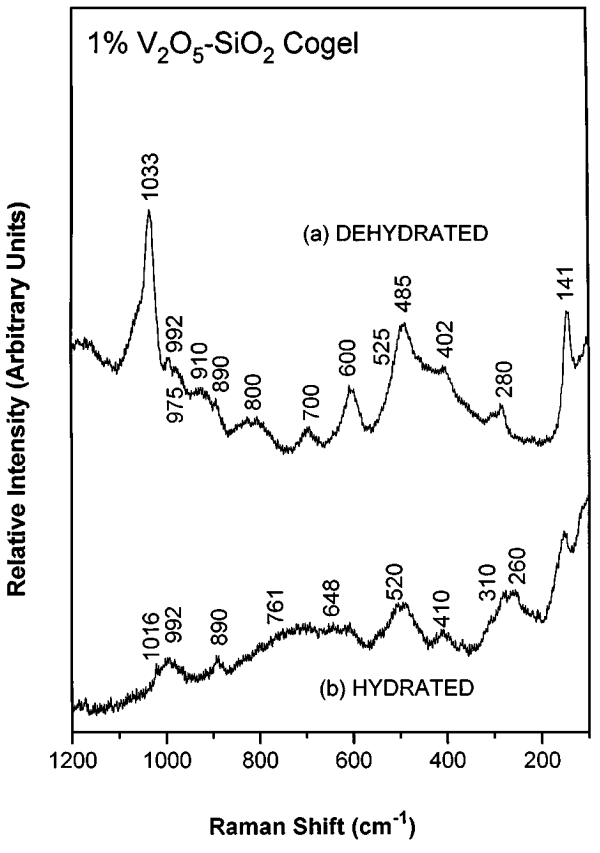

FIG. 3. Raman spectra of 1% V_2O_5-SiO_2 cogel catalyst under (a) dehydrated and (b) hydrated conditions.

The wide-line and MAS ^{51}V NMR spectra of a 10% silica-supported vanadia catalyst have been previously published in Ref. (18). Essentially an identical feature has been observed for the 1% silica-supported vanadia sample but the signal-to-noise ratio is poor due to the low density and fluffy nature of the silica support used. A line centered at ~ -510 ppm with the components of an anisotropic chemical shift tensor at -450, -470, and -1190 ppm in the silica supported samples has been assigned to a distorted surface VO_4 species with a close-to-axial symmetry (18,31). In contrast to the distorted VO_4 species in V-silicalite, the distorted surface VO_4 species in the silica-supported vanadia catalyst is very sensitive to water vapor. Water adsorption leads to coordination change from VO_4 to VO_5 or VO_6, evidenced by the -510 ppm line completely shifting to ~ -300 ppm upon hydration.

The wide-line ^{51}V NMR spectrum of the 1% cogel sample gives a broad line located at ~ -510 ppm with the components of an anisotropic shift tensor at -460, -500, and -850 ppm, which can also be assigned to a distorted VO_4 species with a close-to-axial symmetry (18,31). Different from the silica-supported vanadia catalyst, however, the ^{51}V NMR line at ~ -510 ppm does not completely shift to ~ -300 ppm upon hydration, indicating that only part of the distorted VO_4 species in the vanadia-silica cogel catalyst undergoes coordination change (16).

Temperature-Programmed Reduction

The temperature-programmed reduction profiles for the 1% silica-supported vanadia, 1% vanadia-silica cogel, and V-silicalite catalysts are shown in Fig. 5. For the silica-supported vanadia and cogel samples, the maxima of reduction peaks are located at $\sim 525^\circ$C due to reduction of the surface vanadium oxide species on silica. The maximum of the reduction peak for the V-silicalite is located at $\sim 550^\circ$C. The reduction peak of the V-silicalite exhibits a very broad feature likely due to diffusion limitations.

Methanol Oxidation

The methanol oxidation activities of the catalysts have been normalized to the number of methanol molecules

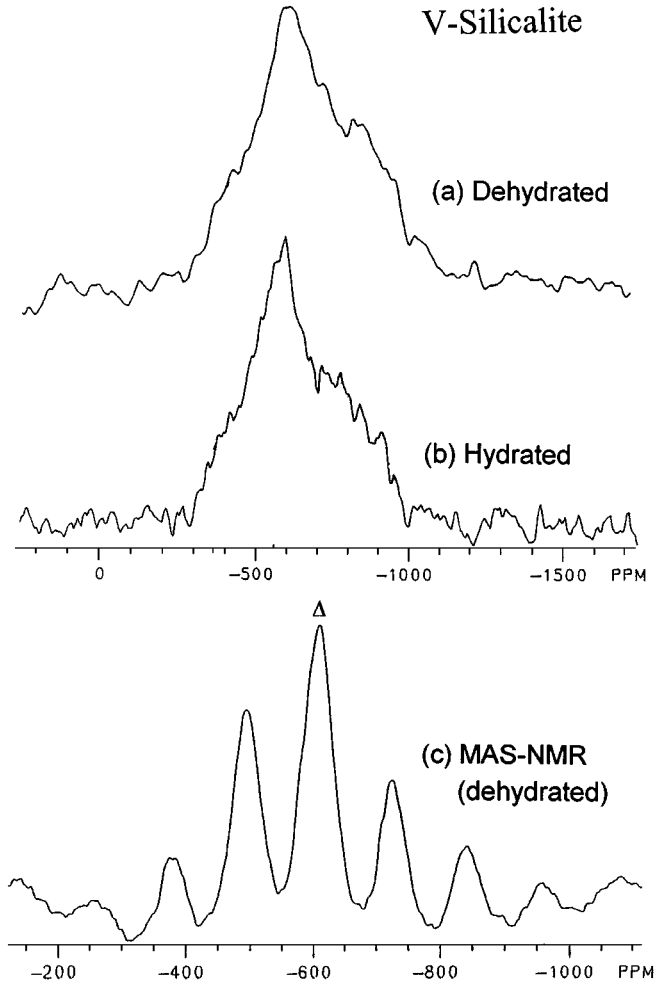

FIG. 4. ^{51}V NMR spectra of V-silicalite: (a) wide-line spectrum under dehydrated conditions; (b) wide-line spectrum under hydrated conditions; and (c) MAS spectrum under dehydrated conditions.

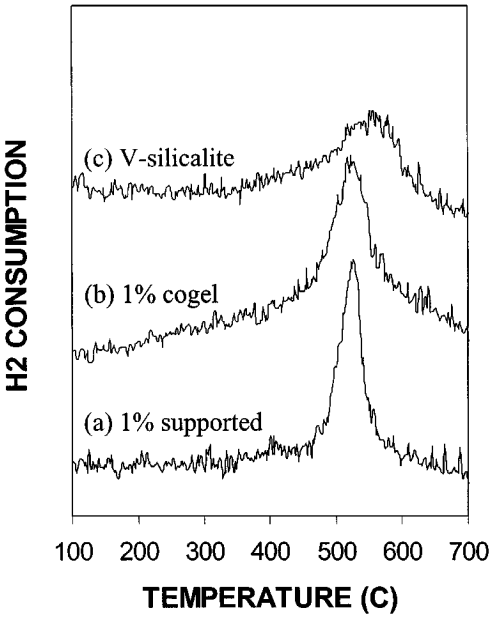

FIG. 5. TPR profiles for: (a) 1% supported V_2O_5/SiO_2; (b) 1% V_2O_5-SiO_2 cogel; and (c) V-silicalite.

converted per dispersed vanadium site per second i.e., the turnover frequency (TOF). The Raman and ^{51}V NMR data have demonstrated that almost ~100% of vanadium are in a dispersed state except a trace of V_2O_5 present in the 1% cogel sample. The methanol conversion, TOFs, and product selectivities of methanol oxidation over the V-silicalite, vanadia-silica cogel, and silica-supported vanadia catalysts are presented in Table 2. The TOFs of the V-silicalite and 1% silica-supported vanadia catalysts are 0.053 and 0.043 s^{-1}, respectively. The TOF (0.028 s^{-1}) of the 1% cogel catalyst is relatively lower than the other two catalysts. All of the catalysts exhibit comparable product selectivities to formaldehyde (84.6–87.0%) and carbon monoxide (12.3–13.0%) at methanol conversion of ~10 mol% at 380°C.

TABLE 2

Activity and Product Selectivities of Methanol Oxidation over 15–45 mg of the Silica-Supported Vanadia, Vanadia-Silica Cogel, and V-Silicalite Catalysts at Atmospheric Pressure and 380°C

Catalyst	Conv. (mol%)	TOF ($\times 1000\ s^{-1}$)	Selectivity (mol%) HCHO	$HCOOCH_3$	CO	CO_2
1% supported	9.1	43	84.6	2.5	12.9	0.0
1% cogel	13.1	28	87.0	0.0	13.0	0.0
V-silicalite	12.9	53	87.0	0.0	12.3	0.7

Note. A gas mixture of methanol/O_2/He = 6/11/83 was used as the feed with a total flow rate of 50 ml/min.

DISCUSSION

Structure of Vanadia Species

The solid-state ^{51}V NMR and Raman studies on vanadia-based catalysts and model compounds with well-defined coordination have been intensively researched over the past decade (17,29,32). Comparison of ^{51}V wide-line NMR line shapes and positions with those of the model compounds has provided much information for determining the local coordination environments of the vanadium species in supported vanadia catalysts. On the basis of dehydrated ^{51}V NMR studies, a distorted VO_4 surface V^{5+} species has been observed on Al_2O_3, TiO_2, and MgO at low vanadia loadings under dehydrated conditions (29–31,33). At high vanadia loadings, both distorted VO_4 and VO_5 (or VO_6) were detected by ^{51}V NMR for these catalysts. The surface V^{5+} species on SiO_2 was determined to contain only a distorted VO_4 coordination at all surface coverages (18,34,35). Furthermore, dehydrated EXAFS (36,37) and Raman (18,19,38) results suggest that the distorted tetrahedral surface V^{5+} species on SiO_2 consists of a single terminal V=O bond characterized by the Raman band at 1037 cm^{-1} and is isolated because no V-O-V neighbor is observed less than 3.5 Å and the vibrations associated with the V-O-V bonds (200–300 and 500–800 cm^{-1}) are not observed. Therefore, the surface vanadia species on silica under dehydrated conditions is an isolated and distorted tetrahedral V^{5+} species with a single V=O bond and three V-O-Si bridging bonds. The surface vanadia species on silica is very sensitive to moisture containing water or methanol. Upon exposure to ambient conditions, the surface vanadia species can change coordination from fourfold to five- or sixfold as evidenced by ^{51}V NMR (18,29) and Raman (18).

The present studies show that only a trace amount of V_2O_5 crystals is present in the 1% cogel because the Raman cross sections of crystalline metal oxides were found to be much stronger than those of surface metal oxide species (39). ^{51}V NMR failed to detect V_2O_5 crystals because ^{51}V NMR technique is not as sensitive as Raman for crystalline V_2O_5. Therefore, the majority of the vanadia species in the cogel is present as a dispersed vanadia species. The Raman feature of the dispersed vanadia species in the 1% cogel sample is essentially the same as that of the 1% silica-supported vanadia catalyst under both hydrated and dehydrated conditions, indicating the presence of the similar surface vanadia species in both the cogel and the silica-supported vanadia catalysts. The NMR spectra further reveal that the dispersed vanadia species in the cogel sample can be divided into two types (A and B) according to their interaction with water. The vanadia species of type A undergoes local coordination change from VO_4 to VO_5 or VO_6 upon hydration; however, the vanadia species of type B retains the VO_4 coordination environment upon hydration. Similar behavior was also documented by Stiegman

and Eckert *et al*. for a 0.5 mol% vanadia-silica xerogel (23). In a separate paper [16], the type A species has been designated as a water-accessible surface vanadia species and the type B as a water-inaccessible surface vanadia species. Previously, an inaccessible vanadia species was found by Lapina *et al.* (35) in silica-supported vanadia catalysts upon calcination at 900°C, where part of the vanadia species was trapped inside SiO_2 due to the collapse of the silica support at high temperatures. Methanol oxidation reveals that the cogel catalyst exhibits lower TOFs than the silica-supported vanadia and V-silicalite catalysts, indicating that the water-inaccessible VO_4 species in the cogel catalyst is not accessible by methanol, either, during the catalytic reaction. These results imply that the type B vanadia species in the cogel sample is trapped inside the closed pores of the catalyst.

The Raman spectrum of the V-silicalite shows significant differences in the 850–1050 cm^{-1} range, compared to that of the pure silicalite, which possesses bands at ca 799–827, 972, and 1085 cm^{-1} in the 700–1100 cm^{-1} region. The bands at ca 799–827 cm^{-1} are associated with the symmetric stretching vibrations of the primary tetrahedral [SiO_4] unit, and the bands at ca 1085 cm^{-1} and above 1200 cm^{-1} originate from the antisymmetric stretching vibrations of the tetrahedral [SiO_4] unit (40). The 972 cm^{-1} band in the pure silicalite has been assigned to a localized ≡Si-OH stretching mode (41–43). Previous Raman studies (44) on Ti-silicalites reveal that the Raman bands at ∼960 and 1115 cm^{-1} cannot be related to Ti-O or Ti=O vibration modes. A systematic Raman study of pure Al-, B-, Ti-, and Fe-substituted silicalites has uncovered that the substitution of Si with Ti, Fe, and B results in the appearance of new Raman active modes at 960 and 1115 cm^{-1} in Ti-silicalite, 1020 cm^{-1} in Fe-silicalite, and 976 and 1417 cm^{-1} in B-silicalite (45). These new Raman bands are assigned to the $[\equiv Si\text{-}O]^{\delta-}$ vibration mode, and the band positions depend on the polarity of the *M*-O-Si bonds (M = Ti, Fe, or B). Similar to Ti-silicalites, the V-silicalite also possesses a broad and intense band centered at ∼960 cm^{-1}. Based on the above discussion, this band is assigned to the stretching vibration modes of the $[\equiv Si\text{-}O]^{\delta-}$ unit perturbed by the presence of V. The Raman bands at 150–300 and 500–800 cm^{-1} due to V-O-V vibrations were not observed, indicating the vanadia species in V-silicalite is isolated.

The weak Raman band at 1034 cm^{-1} in V-silicalite has the same band position as the terminal V=O double bond observed for the surface vanadia oxide species on silica (17,18). Thus, the band at ∼1034 cm^{-1} is assigned to the vibration mode of a terminal V=O bond in the V-silicalite, and its relative intensity is related to the amount of the vanadia species possessing a terminal V=O bond. Therefore, the extremely weak ∼1034 cm^{-1} Raman band in V-silicalite suggests that the vanadia species in the V-silicalite essentially does not possess a terminal V=O bond. In contrast, the Raman feature at 1034 cm^{-1} was extremely intense for another V-silicalite (not shown here), which was synthesized using Ludox AS-40 (Dupont) as the silicon source (21). The 1034 cm^{-1} band of the later V-silicalite sample shifts to the 914–1003 cm^{-1} region upon hydration, evidenced by intensification of the band in the 914–1003 cm^{-1} range and the disappearance of the 1034 cm^{-1} band.

The solid state ^{51}V NMR data listed in Table 1 reveals that the highly distorted VO_4 species is present in the V-silicalite catalyst. Nevertheless, the fourfold coordinated vanadia species is different from the distorted surface VO_4 species on silica. First, the vanadia species in the V-silicalite has a lower symmetry than the vanadia species in the silica-supported catalyst, evidenced from the differences in the components of the chemical shift tensors. Second, the vanadia species in the V-silicalite does not change its coordination environment upon hydration, suggesting that the vanadium is incorporated in the zeolite framework because vanadia species connected to the framework at defect sites forming so-called framework satellites could apparently change its coordination upon hydration. Furthermore, the very intense Raman band at ∼960 cm^{-1} and the slight increase in the unit cell parameters further suggest possible incorporation of V in the silicalite framework in V-silicalite.

There is some debate in the literature on the substitution of vanadium into the silicalite framework (46a,46b). For V-silicalites with the MEL structure, evidence about the framework substitution by V was from the direct correlation between vanadium content and unit cell parameters (14,46a). The relative intensity of the ∼960 cm^{-1} IR band also increased linearly with the vanadium content and the unit cell volume (46a). For V-silicalites with the MFI structure, however, such a correlation between vanadium content and unit cell parameters was not available in the literature (21,22,46b).

In summary, four V^{5+} species can be distinguished from the ^{51}V NMR and Raman studies in the dehydrated V-silicalite, vanadia-silica cogel, and silica-supported vanadia catalysts:

(1) crystalline V_2O_5 in the vanadia-silica cogel sample, which possesses a distorted V^{5+} with fivefold coordination;

(2) an isolated and distorted V^{5+} species possessing fourfold coordination with a terminal V=O bond and three V-O-Si bridge bonds, which changes coordination upon hydration and is present in the silica-supported vanadia and cogel catalysts;

(3) an isolated and distorted V^{5+} species possessing fourfold coordination, which is present in the cogel sample and inaccessible to water and methanol;

(4) an isolated and highly distorted V^{5+} species possessing fourfold coordination essentially without a terminal V=O bond is present in the V-silicalite and does not change coordination upon hydration.

Reducibility and Reactivity of Vanadia Sites

There are a few studies focused on temperature-programmed reduction of silica-supported vanadia catalysts in the literature (47,48). Roozeboom *et al.* assigned a reduction peak at 430°C to a surface vanadia phase and a second peak at 430–510°C to crystalline V_2O_5 (47). Similarly, Koranne *et al.* attributed a peak (p_1) at 460°C to a surface species and the peaks at 540°C (p_2) and 580°C (p_3) to a combination of reduction peaks corresponding to various reduction states of "bulk-like" vanadia on the silica support (48). In this work, only the surface VO_4 species is present in the 1% silica-supported vanadia catalyst under dehydrated conditions, suggesting that the peak at 525°C should be assigned to the surface VO_4 species on silica. Similarly, the reduction peak at 525°C in the 1% cogel sample is also due to the surface VO_4 species. The Raman and NMR results showed that the VO_4 species in the V-silicalite sample is highly dispersed without crystalline V_2O_5. Thus, the reduction peak at 550°C in V-silicalite comes from reduction of the highly dispersed VO_4 species. Compared to that of the surface VO_4 species in the silica-supported catalyst, the reduction peak of the V-silicalite is very broad and shifts to slightly higher temperature because of diffusion limitations in the V-silicalite sample. The TPR studies reveal that the dispersed vanadia species in the silica-supported, cogel, and V-silicalite catalysts essentially possess similar reducibility.

Methanol oxidation has been established as a reliable chemical probe of metal oxide catalysts through comparison of catalytic activity and product selectivities (49). The catalytic data presented in Table 2 show that the V-silicalite, vanadia-silica cogel, and silica-supported vanadia catalysts exhibit comparable TOFs and selectivity patterns. Similar catalytic results were previously reported for methanol oxidation over Ti-silicalites and silica-supported titania catalysts (44) and for vapor phase toluene oxidation over VAPO-5, V-silicalite, V-ZSM-5, and V-aerosil 90 (50). However, the utility of different oxide supports (e.g., TiO_2, Al_2O_3, CeO_2) results in four orders of magnitude variation in the methanol oxidation TOFs over these supported vanadia catalysts (17,51). The current findings correspond to the previous conclusion that methanol oxidation TOFs primarily correlate with the bridging V-O-support bonds of the supported vanadia catalysts (17,51). Pure silica exhibits low activity and gives carbon oxides as the main products (52). The formation of formaldehyde, a selective oxidation product, corresponds to the dispersed V^{5+} species. As discussed above, all the vanadia catalysts in the different silica environments contain isolated and distorted V^{5+} species with the bridging V-O-Si bonds that are the active functionality for methanol oxidation. Thus, the vanadia species exhibit similar reactivity no matter whether vanadium is anchored onto the amorphous silica surface or incorporated into the silicalite framework because Si is the only ligand in all cases and no matter whether the VO_4 species contain a terminal V=O bond. The prior studies have concluded that the terminal V=O bond does not play a critical role during methanol oxidation over supported vanadia catalysts (17,52).

The stability of the vanadia species in the V-silicalite, vanadia-silica cogel, and silica-supported vanadia catalysts is different in the presence of water or methanol. The vanadium loss of the silica-supported vanadia and cogel catalysts during methanol oxidation was found to be significant, especially for the catalysts with high vanadia loadings. The V-silicalite catalyst exhibits higher stability against water and methanol moistures. Similar conclusions were also reached for Ti-silicalite catalysts (44). Consequently, all the catalysts exhibit similar catalytic properties in vapor-phase reactions, but different stabilities.

CONCLUSIONS

The highly dispersed vanadia species in different silica environments (silicalite, cogel, and silica-supported) under dehydrated conditions possess an isolated and distorted fourfold coordination with minor differences. The vanadia species in the silica-supported vanadia catalyst possesses a terminal V=O bond and is very sensitive to moisture, which leads to coordination change from a fourfold to five- or sixfold environment. The vanadia species in the V-silicalite essentially does not change coordination upon hydration and does not appear to have a terminal V=O bond. The vanadia-silica cogel has a trace amount of crystalline V_2O_5 and two types of dispersed vanadia species; one is the surface vanadia species on silica. All the dispersed vanadia species in the different silica environments exhibit similar reducibility and catalytic properties for methanol oxidation because they possess similar bridging V-O-Si bonds that are critical for catalysis of methanol oxidation and reduction of these species.

ACKNOWLEDGMENTS

The financial support of NSF (Grant CTS-9417981) is gratefully acknowledged. The authors thank Dr. M. S. Rigutto, Dr. H. van Bekkum, Dr. K. Klier, Dr. R. G. Herman, Xingtao Gao, Dr. H. Eckert, Dr. A. Turek, and Dr. Bert Weckhuysen for providing samples and/or characterization information.

REFERENCES

1. Koranne, M. M., Goodwin, J. G., Jr., and Marcelin, G., *J. Catal.* **148**, 388 (1994).
2. Oyama, S. T., Middlebrook, A. M., and Sormorjai, G. A., *J. Phys. Chem.* **94**, 5029 (1990).
3. Takenaka, S., Kuriyama, T., Tanaka, T., Funabiki, T., and Yoshida, S., *J. Catal.* **155**, 196 (1995).
4. Owens, L., and Kung, H. H., *J. Catal.* **144**, 202 (1993).
5. Bellussi, G., Centi, G., Perathoner, S., and Trifiro, F., *ACS Symp. Ser.* **523**, 281 (1996).

6. Tatsumi, T., Hirasawa, Y., and Tsuchiya, J., *ACS Symp. Ser.* **638**, 374 (1996).
7. Habersberger, K., Jiru, P., Tvaruzkova, Z., Centi, G., and Trifiro, F., *React. Kinet. Catal. Lett.* **39**, 95 (1989).
8. Mal, N. K., and Ramaswamy, A. V., *Appl. Catal. A* **143**, 75 (1996).
9. Reddy, J. S., and Sayari, A., *Catal. Lett.* **28**, 263 (1994).
10. Zatorki, L. W., Centi, G., Lopez Nieto, N., Trifiro, F., Bellussi, G., and Fattore, V., *in* "Zeolites: Facts, Figures, Future" (P. A. Jacobs and R. A. van Stanten, Eds.), p. 1243. Elsevier Science, Amsterdam, 1989.
11. Cavani, F., Trifiro, F., Jiru, P., Habersberger, K., and Tvaruzkova, Z., *Zeolites* **8**, 12 (1988).
12. Miyamoto, A., Medhanavyn, D., and Inui, T., *in* "Proc. 9th Intern. Congr. Catal." (M. J. Phillips, Ed.), Vol. 1, p. 437. Chemical Institute of Canada, Ottawa, Canada, 1988.
13. Whittington, B. I., and Anderson, J. R., *J. Phys. Chem.* **95**, 3306 (1991).
14. Hari Prasad Rao, P. R., Belhekar, A. A., Egde, S. H., Ramaswamy, A. V., and Ratnasamy, P., *J. Catal.* **141**, 595 (1993).
15. Baiker, A., Dollenmeier, P., Glinski, M., Reller, A., and Sharma, V. K., *J. Catal.* **111**, 273 (1988).
16. Wang, C. B., Herman, R. G., Shi, C., Sun, Q., Klier, K., and Roberts, J. E., to be published.

17a. Deo, G., Wachs, I. E., and Haber, J., *Critical Rev. Surf. Chem.* **4**, 141 (1994).

17b. Wachs, I. E., and Weckhuysen, B. M., *Appl. Catal: General A* **157**, 67 (1997).

17c. Wachs, I. E., *in* "Catalysis" (J. J. Spivey, Ed.), Vol. 13, 37. The Royal Society of Chemistry, Cambridge, 1997.

18. Das, N., Eckert, H., Hu, H., Wachs, I. E., Walzer, J. F., and Feher, F. J., *J. Phys. Chem.* **97**, 8240 (1993).
19. Went, G. T., Oyama, S. T., and Bell, A. T., *J. Phys. Chem.* **94**, 4240 (1990).
20. Anpo, M., Sunamoto, M., and Che, M., *J. Phys. Chem.* **93**, 1187 (1993).
21. Rigutto, M. S., and van Bekkum, H., *Appl. Catal.* **68**, L1 (1991).
22. Centi, G., Perathoner, S., Trifiro, F., Aboukais, A., Aissi, C. F., and Guelton, M., *J. Phys. Chem.* **96**, 2617 (1992).
23. Stiegman, A. E., Eckert, H., Plett, G., Kim, S. S., Anderson, M., and Yavrouian, A., *Chem. Mat.* **5**, 1591 (1993).
24. Wachs, I. E., Hardcastle, F. D., and Chan, S. S., *Spectroscopy* **1**, 30 (1986).
25. Chan, S. S., Wachs, I. E., Murrell, L. L., Wang, L., and Hall, W. K. *J. Phys. Chem.* **88**, 5831 (1984).
26. Deo, G., and Wachs, I. E., *J. Catal.* **146**, 335 (1994).

27a. van Koningsveld, H., van Bekkum, H., and Jansen, J. C., *Acta Cryst. B* **43**, 123 (1987).

27b. Flanigen, E. M., Bennett, J. M., Grose, R. W., Cohen, J. P., Patton, R. L., Kirchner, R. M., and Smith, J. V., *Nature* **271**, 512 (1978).

28. Oyama, S. T., Went, G. T., Lewis, K. B., Bell, A. T., and Somorjai, G. A., *J. Phys. Chem.* **93**, 6786 (1989).
29. Lapina, O. B., Mastikhin, V. M., Shubin, A. A., Kradilnikov, V. N., and Zamaraev, K. I., *Progr. NMR Spectrosc.* **24**, 457 (1992).
30. Eckert, H., and Wachs, I. E., *J. Phys. Chem.* **93**, 6796 (1989).
31. Le Coustumer, L. R., Taouk, B., Le Meur, M., Payen, E., Guelton, M., and Grimblot, J., *J. Phys. Chem.* **92**, 1230 (1988).
32. Bond, G. C., and Tahir, S. F., *Appl. Catal.* **71**, 1 (1991).
33. Lapina, O. B., Simakov, A. V., Mastikhin, V. M., Veniaminov, S. A., and Shibin, A. A., *J. Mol. Catal.* **50**, 55 (1989).
34. Taouk, B., Guelton, M., Grimblot, J., and Bonnelle, J. P., *J. Phys. Chem.* **92**, 6700 (1988).
35. Lapina, O. B., Mastikhin, V. M., Nosov, A. V., Beutel, T., and Knozinger, H., *Catal. Lett.* **13**, 203 (1992).
36. Yoshida, S., Tanaka, T., Nishimura, Y., Mizutani, H., and Funabiki, T., *in* "Proc. 9th Intern. Congr. Catal." (M. J. Phillips, Ed.), Vol. 3, p. 1473. Chemical Institute of Canada, Ottawa, Canada, 1988.
37. Yoshida, S., Tanaka, T., Hanada, T., Hiraiwa, T., and Kanai, H., *Catal. Lett.* **12**, 277 (1992).
38. Hardcastle, F. D., and Wachs, I. E., *J. Phys. Chem.* **95**, 5031 (1991).
39. Chan, S. S., Wachs, I. E., and Murrell, L. L., *J. Catal.* **90**, 150 (1984).
40. Miecznikowski, A., and Hanuza, J., *Zeolites* **7**, 249 (1987).
41. Zecchina, A., Bordiga, S., Spoto, S., Marchese, L., Petrini, G., Leofanti, G., and Padovan, M., *J. Phys. Chem.* **96**, 4985 (1992); 4991 (1992).
42. Tallant, D. R., Bunker, B. C., Brinker, C. J., and Balfe, C. A., *Mat. Res. Soc. Symp. Proc.* **73**, 261 (1886).
43. Stolen, R. H., and Walfen, G. E., *J. Chem. Phys.* **64**, 2623 (1976).
44. Deo, G., Turek, A. M., Wachs, I. E., Huybrechts, A. R. C., and Jacobs, P. A., *Zeolites* **13**, 365 (1993).
45. Scarano, D., Zecchina, A., Bordiga, S., Geobaldo, F., Spoto, G., Petrini, G., Leofanti, G., Padovan, M., and Tozzola, G., *J. Chem. Soc. Faraday Trans.* **89**, 4123 (1993).

46a. Hari Prasad Rao, P. R., Kumar, R., Pamaswamy, A. V., and Ratnasamy, P., *Zeolites* **13**, 663 (1993).

46b. Bellussi, G., and Rigutto, M. S., *Stud. Surf. Sci. Catal.* **85**, 177 (1994).

47. Roozeboom, F., Mittelmeijer-Hazeleger, M. C., Moulijn, J. A., Medema, J., de Beer, V. H. J., and Gellings, P. J., *J. Phys. Chem.* **84**, 2783 (1980).
48. Koranne, M. M., Goodwin, J. G., Jr., and Marcelin, G., *J. Catal.* **148**, 369 (1994).
49. Tatibouet, J. M., *Appl. Catal. A* **148**, 213 (1997).
50. Whittington, B. I., and Anderson, J. R., *J. Phys. Chem.* **97**, 1032 (1993).
51. Wachs, I. E., Deo, G., Juskelis, M., and Wechhuysen, B. M., *in* "Dynamics of Surfaces and Reaction Kinetics in Heterogeneous Catalysis" (G. F. Froment and K. C. Waugh, Eds.), p. 305. Elsevier Science, Amsterdam, 1997.
52. Jehng, J. M., Hu, J., Gao, X., and Wachs, I. E., *Catal. Today* **28**, 335 (1996).